Bcl-2 differentially regulates Ca^{2+} signals according to the strength of T cell receptor activation

Fei Zhong,[1] Michael C. Davis,[1,2] Karen S. McColl,[1] and Clark W. Distelhorst[1,2,3,4]

[1]Department of Medicine, [2]Department of Pharmacology, and [3]Comprehensive Cancer Center, Case Western Reserve University, and [4]University Hospitals of Cleveland, Cleveland, OH 44106

To investigate the effect of Bcl-2 on Ca^{2+} signaling in T cells, we continuously monitored Ca^{2+} concentration in Bcl-2–positive and –negative clones of the WEHI7.2 T cell line after T cell receptor (TCR) activation by anti-CD3 antibody. In Bcl-2–negative cells, high concentrations of anti-CD3 antibody induced a transient Ca^{2+} elevation, triggering apoptosis. In contrast, low concentrations of anti-CD3 antibody induced Ca^{2+} oscillations, activating the nuclear factor of activated T cells (NFAT), a prosurvival transcription factor. Bcl-2 blocked the transient Ca^{2+} elevation induced by high anti-CD3, thereby inhibiting apoptosis, but did not inhibit Ca^{2+} oscillations and NFAT activation induced by low anti-CD3. Reduction in the level of all three inositol 1,4,5-trisphosphate ($InsP_3$) receptor subtypes by small interfering RNA inhibited the Ca^{2+} elevation induced by high but not low anti-CD3, suggesting that Ca^{2+} responses to high and low anti-CD3 may have different requirements for the $InsP_3$ receptor. Therefore, Bcl-2 selectively inhibits proapoptotic Ca^{2+} elevation induced by strong TCR activation without hindering prosurvival Ca^{2+} signals induced by weak TCR activation.

Introduction

Ca^{2+} is a versatile second messenger that mediates a wide range of cellular processes, including cell division and apoptosis (Berridge et al., 2003). Under physiological conditions, cytoplasmic Ca^{2+} is maintained at a low level, and it is the elevation of cytoplasmic Ca^{2+} that generates Ca^{2+} signals. Elevated Ca^{2+} transmits information by activating Ca^{2+}-sensitive effectors, including phosphatases and kinases. The Ca^{2+} elevation involved in signal transduction is often in the form of repetitive Ca^{2+} spikes or oscillations (Berridge, 1997b). The information-processing capability of Ca^{2+} signaling is enhanced by modulation of the frequency, amplitude, and spatial properties of Ca^{2+} elevations. This in part explains how a simple messenger such as Ca^{2+} can regulate diverse cellular processes.

In T cells, Ca^{2+} signals mediate a variety of responses to T cell receptor (TCR) activation, including cell proliferation and apoptosis (Winslow et al., 2003; for reviews see Berridge, 1997a; Lewis, 2001, 2003; Randriamampita and Trautmann, 2004). As in all nonexcitable cells, the T cell Ca^{2+} response begins with the release of Ca^{2+} from the ER through inositol 1,4,5-trisphosphate ($InsP_3$)–dependent Ca^{2+} channels ($InsP_3$ receptors). The resulting cytoplasmic Ca^{2+} elevation is amplified by Ca^{2+} entry through Ca^{2+}-release–activated Ca^{2+} channels on the plasma membrane, producing either a transient Ca^{2+} elevation or Ca^{2+} oscillations (Donnadieu et al., 1992a,b; Hess et al., 1993; for review see Lewis, 2001). The Ca^{2+} signal is then transduced through Ca^{2+}/calmodulin–mediated activation of the protein phosphatase calcineurin, which dephosphorylates and thereby activates the nuclear factor of activated T cells (NFAT; for review see Lewis, 2003; Winslow et al., 2003). NFAT is a transcription factor that activates the interleukin-2 promoter, increasing cell proliferation. Activation of calcineurin, and hence NFAT, is sustained more efficiently by Ca^{2+} oscillations than by a transient elevation of Ca^{2+}, whereas other Ca^{2+} responses (e.g., nuclear factor kB and c-Jun NH_2-terminal kinase activation) are preferentially activated by transient Ca^{2+} elevation (Dolmetsch et al., 1997, 1998). The importance of Ca^{2+} oscillations in T cell signaling is increasingly recognized, including evidence that Ca^{2+} oscillations regulate thymocyte motility during positive selection in the thymus (Bhakta et al., 2005).

We recently reported that the antiapoptotic protein Bcl-2 (Cory and Adams, 2002) interacts with $InsP_3$ receptors on the ER and inhibits $InsP_3$-mediated Ca^{2+} efflux (Chen et al., 2004). As a consequence, Bcl-2 dampens the cytoplasmic Ca^{2+} elevation induced by an antibody to the CD3 component of the TCR complex. These findings are intriguing in view of the known role of Ca^{2+} in signaling apoptosis (for reviews see Hajnoczky et al., 2003; Orrenius et al., 2003; Hanson et al., 2004), but an

F. Zhong and M.C. Davis contributed equally to this paper.

Correspondence to Clark W. Distelhorst: cwd@case.edu

Abbreviations used in this paper: $InsP_3$, inositol 1,4,5-trisphosphate; NFAT, nuclear factor of activated T cells; siRNA, small interfering RNA; TCR, T cell receptor.

The Journal of Cell Biology, Vol. 172, No. 1, January 2, 2006 127–137
http://www.jcb.org/cgi/doi/10.1083/jcb.200506189

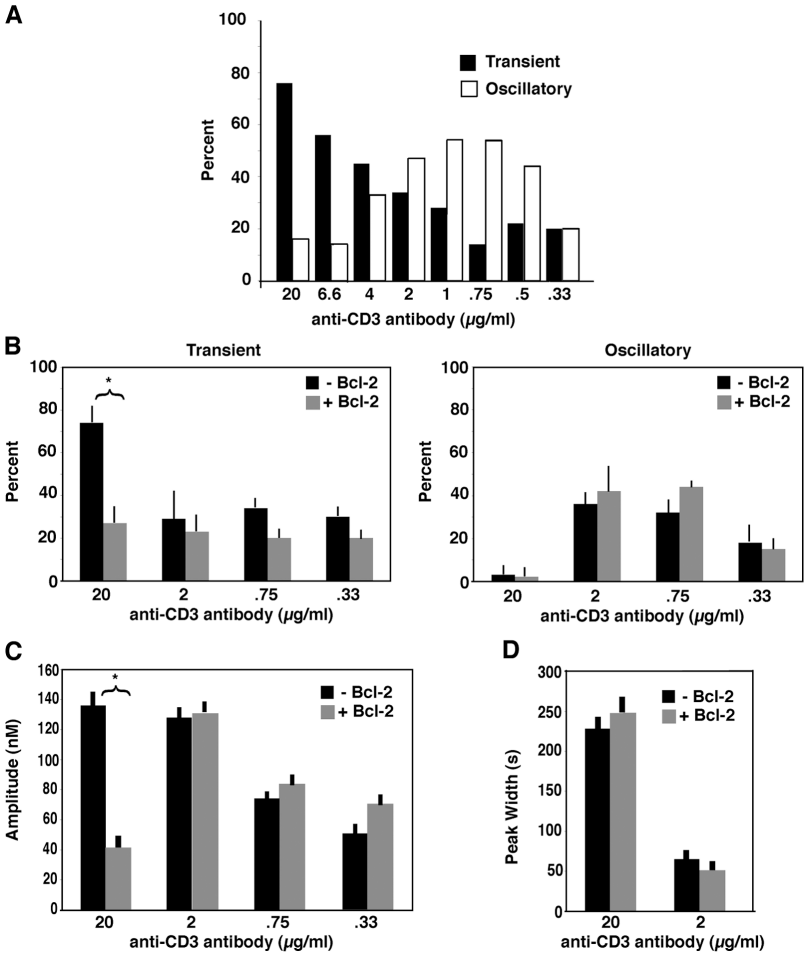

Figure 1. **Ca^{2+} responses to high and low anti-CD3 differ and are differentially regulated by Bcl-2.** (A) Cytoplasmic Ca^{2+} was continuously monitored by digital imaging in Bcl-2–negative WEHI7.2 cells (clone N2) before and after addition of anti-CD3 antibody (experiments 110504–111904). Bars represent the percentage of cells on a single coverslip (~50 cells per coverslip) that developed either a transient elevation of Ca^{2+} or sustained oscillations at each anti-CD3 concentration. In control experiments, no Ca^{2+} elevation was detected in the absence of anti-CD3 treatment (not depicted). (B) Cytoplasmic Ca^{2+} was monitored continuously by digital imaging in Bcl-2–negative and –positive cells after addition of anti-CD3 antibody at the concentrations shown. Bars represent the percentage of cells developing either a transient Ca^{2+} elevation (left) or Ca^{2+} oscillations (right). Error bars represent the mean ± SEM of multiple experiments (20 μg/ml: 6 experiments, mean 40 cells per experiment; 2 μg/ml: 24 experiments in Bcl-2–negative cells, mean 25 cells per experiment, and 22 experiments in Bcl-2–positive cells, mean 33 cells per experiment; 0.75 μg/ml: 7 experiments in Bcl-2–negative cells, mean 53 cells per experiment, and 6 experiments in Bcl-2–positive cells, mean 39 cells per experiment; 0.33 μg/ml: 4 experiments for Bcl-2–negative cells, mean 60 cells per experiment, and 4 experiments for Bcl-2–positive cells, mean 54 cells per experiment). (C) The peak amplitude of each Ca^{2+} elevation induced by the different concentrations of anti-CD3 antibody is summarized based on the same experiments as in B. (D) The width of transient elevations induced by 20 μg/ml anti-CD3 and both transient elevations and oscillatory spikes induced by 2 μg/ml anti-CD3 were recorded. The width was measured at one third of the peak height. Data are from experiments 110804N2 (29 transient elevations) and 110504B17 (19 transient elevations) at 20 μg/ml and experiments 110804N2 (119 elevations) and 110804B17 (66 elevations) at 2 μg/ml anti-CD3. Data from three Bcl-2–negative clones (N2, -10, and -11) and three Bcl-2–positive clones (B6, -9, and -17) were in agreement and therefore were combined in B–D. Error bars represent mean ± SEM. Asterisks designate a statistically significant difference ($P < 0.01$).

inhibitory effect of Bcl-2 on $InsP_3$-mediated Ca^{2+} elevation would seem incompatible with the wide range of physiological processes governed by $InsP_3$-mediated Ca^{2+} signals. Would not Bcl-2 interfere with Ca^{2+} signals that regulate physiological processes required for cell function and survival?

A possible clue to this dilemma was provided by earlier work indicating that Ca^{2+} responses after TCR activation vary according to the strength of TCR activation (Donnadieu et al., 1992a). Typically, strong signals induced by a high concentration of anti-CD3 antibody trigger a single transient elevation of cytoplasmic Ca^{2+}, whereas weaker signals induced by a low concentration of anti-CD3 induce Ca^{2+} oscillations (Donnadieu et al., 1992a). Our previous experiments demonstrating an inhibitory effect of Bcl-2 on anti-CD3–induced Ca^{2+} elevation used a high concentration of anti-CD3 antibody that induced a transient Ca^{2+} elevation rather than Ca^{2+} oscillations. Therefore, in the present work, we investigated the effect of Bcl-2 on Ca^{2+} signals induced over a broad range of anti-CD3 concentrations. This led to the discovery that Bcl-2 differentially regulates Ca^{2+} signals according to the strength of TCR activation. Thus, Bcl-2 inhibited the transient Ca^{2+} elevation induced by a high concentration of anti-CD3 antibody, without interfering with Ca^{2+} oscillations induced by a low concentration of anti-CD3 antibody. Accordingly, Bcl-2 inhibited Ca^{2+}-mediated apoptosis after strong TCR activation but did not inhibit NFAT activation after weak TCR activation. Therefore, by selectively regulating Ca^{2+} signals according to the strength of TCR activation, Bcl-2 discriminates between proapoptotic and prosurvival Ca^{2+} signals.

Results

Bcl-2 inhibits Ca^{2+} elevation induced by high but not low anti-CD3 antibody

The WEHI7.2 T cell line corresponds to an immature double-positive stage of T cell differentiation, as WEHI7.2 cells express both CD4 and -8 antigens and are sensitive to glucocorticosteroid-induced apoptosis. Consistent with this stage of development, Bcl-2 is virtually undetectable in WEHI7.2 cells. In earlier work, Bcl-2–positive and –negative clones were derived by stably transfecting WEHI7.2 cells with an expression vector encoding full-length human Bcl-2 or an empty vector, respectively. The full characterization of the clones used in this work has been reported previously (Chen et al., 2004). All findings reported here are based on comparison of three Bcl-2–positive and three Bcl-2–negative clones. Findings were consistent

among the different clones; therefore, data from individual clones have been pooled, unless otherwise noted.

Throughout this paper, cytoplasmic Ca^{2+} was measured at a single-cell level by digital imaging. An initial series of Ca^{2+} measurements was performed to determine the dose–response relationship between anti-CD3 concentration and cytoplasmic Ca^{2+} response patterns in a Bcl-2–negative clone (Fig. 1 A). In this experiment, a transient elevation of Ca^{2+} was defined as only one or two Ca^{2+} elevations reaching at least twice the basal level of Ca^{2+}, whereas sustained Ca^{2+} oscillations were defined as three or more Ca^{2+} spikes at least twice the basal level of Ca^{2+} and separated by at least a 30-s interval. The percentage of cells responding with a transient Ca^{2+} elevation was maximal at 20 μg/ml anti-CD3 antibody and declined progressively with increasing antibody dilution (Fig. 1 A). Conversely, the percentage of cells developing Ca^{2+} oscillations increased progressively as anti-CD3 antibody concentration was reduced. Thus, there is a reciprocal dose–response relationship for transient elevations of Ca^{2+} versus Ca^{2+} oscillations after TCR activation. Based on these initial findings, subsequent studies used 20 μg/ml as representative of a high concentration of anti-CD3 antibody and 2, 0.75, and 0.33 μg/ml as representative of low concentrations of anti-CD3 antibody.

Representative Ca^{2+} traces comparing Bcl-2–negative and –positive cells at a high anti-CD3 concentration (20 μg/ml) are shown in Fig. 2. Bcl-2–negative cells responded to high anti-CD3 with an almost synchronous elevation of cytoplasmic Ca^{2+} as shown in Fig. 2 A, where multiple single-cell Ca^{2+} traces collected in a single experiment (i.e., a single microscope coverslip) are plotted together. In contrast, only a small proportion of Bcl-2–positive cells responded with a detectable Ca^{2+} elevation (Fig. 2 E). The inhibitory effect of Bcl-2 on anti-CD3–induced Ca^{2+} elevation in these experiments is also illustrated by averaging the Ca^{2+} response of multiple cells (Fig. 2, B and F). Characteristics of Ca^{2+} responses at a single-cell level are illustrated by the Ca^{2+} traces in Fig. 2 (C, D, G, and H). Though the number of responding cells and the amplitude of Ca^{2+} elevations differed markedly between Bcl-2–negative and –positive cells, the shape of the Ca^{2+} elevation was similar. In a small percentage of cells, secondary Ca^{2+} elevations were observed (e.g., Fig. 2 H), but as noted in Fig. 1 B, sustained oscillations were infrequent.

Representative Ca^{2+} traces comparing Bcl-2–negative and –positive cells at lower concentrations of anti-CD3 antibody (2, 0.75, and 0.33 μg/ml) are shown in Fig. 3. In contrast to the broad elevation of Ca^{2+} triggered at 20 μg/ml anti-CD3, the Ca^{2+} responses at low concentrations of anti-CD3 antibody were typically in the form of narrow spikes. Also, in contrast to the inhibitory effect of Bcl-2 on Ca^{2+} responses at high anti-CD3, Bcl-2 did not inhibit the Ca^{2+} spikes evoked by low concentrations of anti-CD3. This is illustrated by the representative traces shown in Fig. 3. In Fig. 3, B–D and F–H show repetitive Ca^{2+} spikes, or oscillations, detected in both Bcl-2–negative and –positive cells over the range of anti-CD3 concentrations tested, whereas A and E show cells where only one or two Ca^{2+} spikes were detected. Note that the Ca^{2+} oscillations induced by low anti-CD3 were irregular in terms of both amplitude and

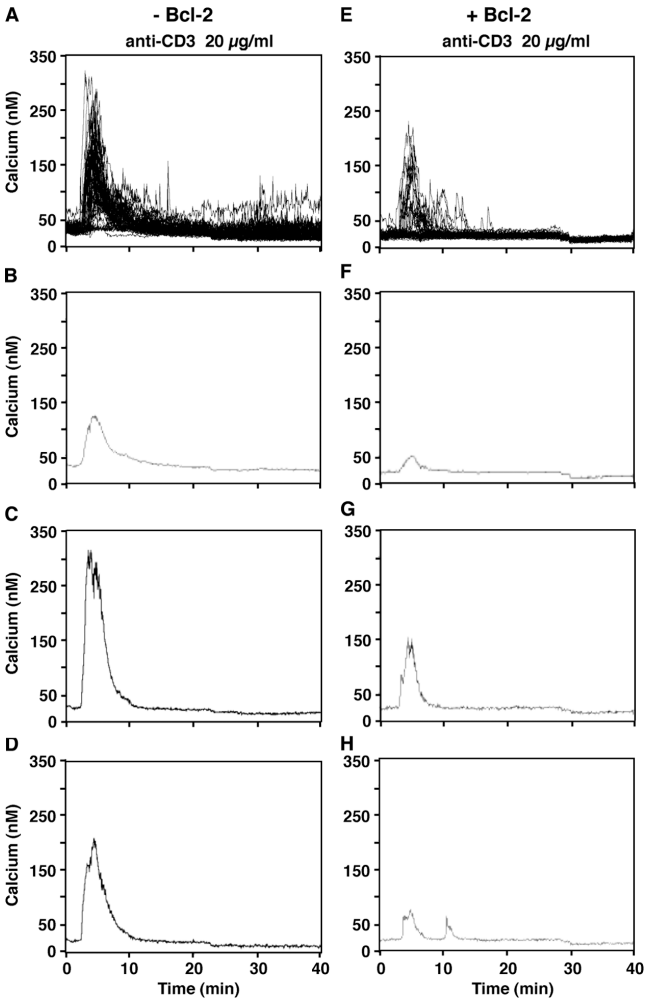

Figure 2. **Bcl-2 inhibits the transient Ca^{2+} elevation induced by high anti-CD3 antibody.** Cytoplasmic Ca^{2+} was continuously monitored by digital imaging in Bcl-2–negative (clone N10) and –positive (clone B6) cells before and after addition of 20 μg/ml anti-CD3 antibody (experiments 022305N10 and 022305B6). Antibody was added during the first 2 min of the trace. (A–D) Bcl-2–negative cells; (E–H) Bcl-2–positive cells. (A) Combined single-cell Ca^{2+} traces from a total of 51 cells on a single coverslip. (E) Combined single-cell Ca^{2+} traces from a total of 53 cells on a single coverslip. (B and F) Mean Ca^{2+} trace for the cells in A and E, respectively. (C, D, G, and H) Single-cell Ca^{2+} traces, illustrating the range of amplitudes of the transient Ca^{2+} elevations obtained at this high anti-CD3 concentration in Bcl-2–negative cells (C and D) and the reduced amplitude of Ca^{2+} transients in Bcl-2–positive cells (G and H). Single-cell traces were from experiments 022305N10 (cells AB and AM) and 022305B6 (cells K and J).

frequency. This is characteristic of Ca^{2+} oscillations in T cells, as reported previously, and is in contrast to the more uniform pattern of Ca^{2+} oscillations observed in nonlymphoid cells (for reviews see Lewis, 2001; Randriamampita and Trautmann, 2004). Also, spontaneous Ca^{2+} oscillations were not detected in control experiments where anti-CD3 was not added to cells.

The responses of cells to either high (20 μg/ml) or low (2, 0.75, or 0.33 μg/ml) anti-CD3 in a large number of experiments are summarized in Fig. 1 (B and C). These data indicate that oscillations are much more frequent at the low than at the high concentration of anti-CD3 (Fig. 1 B). Moreover, these data

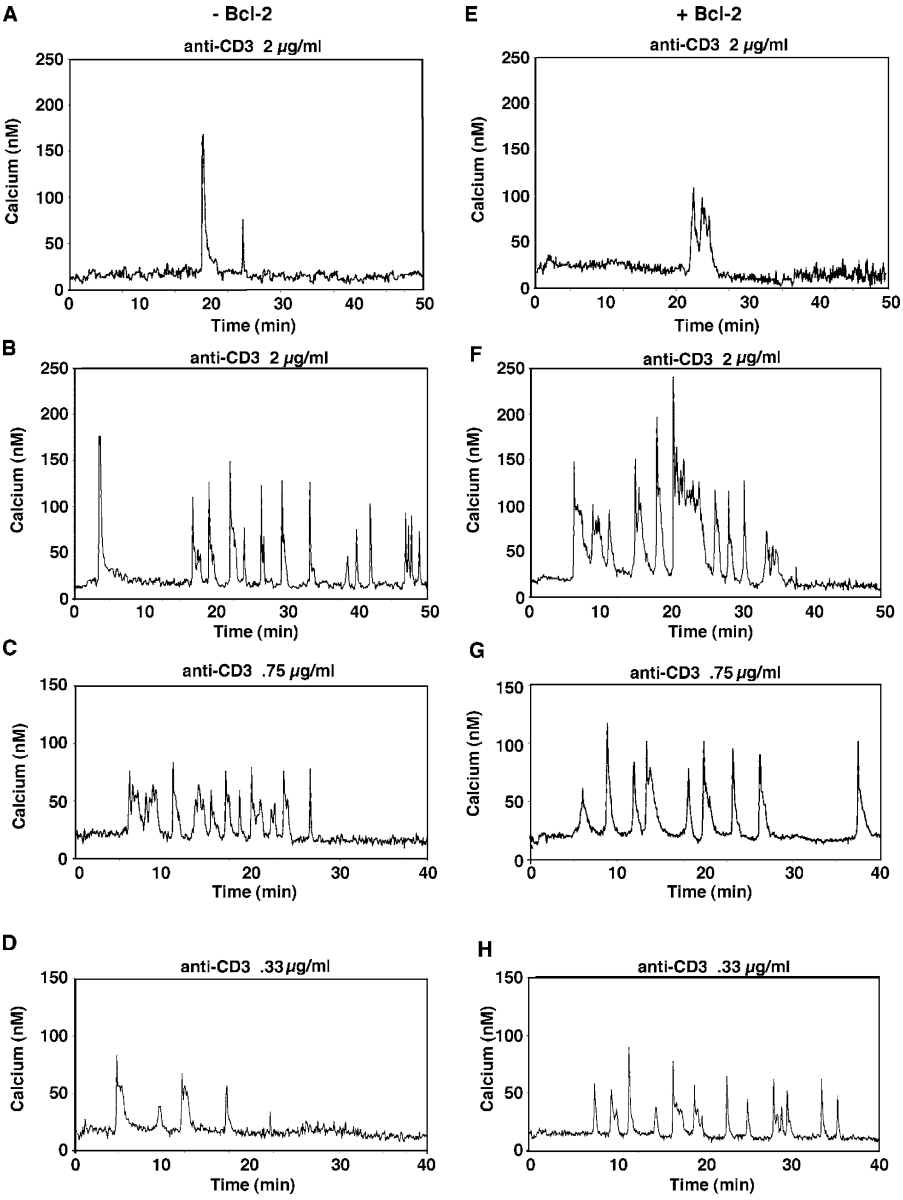

Figure 3. **Bcl-2 does not inhibit Ca^{2+} oscillations induced by low anti-CD3 antibody.** Cytoplasmic Ca^{2+} was continuously monitored by digital imaging in Bcl-2–negative (A–D) and –positive (E–H) cells before and after addition of 2, 0.75, or 0.33 μg/ml anti-CD3 antibody. Antibody was added during the first 2 min of the trace. A and E illustrate cells with only two Ca^{2+} spikes, whereas B–D and F–H illustrate sustained Ca^{2+} oscillations (three or more spikes). Links to original data files are as follows: A, 090104N11, cell AA; B, 090104N11, cell AI; C, 080505, cell BG; D, 082305, cell G; E, 070104, cell H; F, 070104, cell K; G, 080505, cell G; H, 082405, cell AE.

confirm that Bcl-2 markedly inhibits Ca^{2+} responses to strong TCR activation (20 μg/ml anti-CD3 antibody), based on a significant ($P \leq 0.01$) reduction in both the percentage of cells that respond (Fig. 1 B) and the amplitude of Ca^{2+} elevations in those cells that do respond (Fig. 1 C). In contrast, Bcl-2 did not inhibit Ca^{2+} responses to weak TCR activation (2, 0.75, or 0.33 μg/ml anti-CD3 antibody), based on the percentage of cells that respond (Fig. 1 B) and the mean amplitude of Ca^{2+} spikes (Fig. 1 C). Interestingly, at low anti-CD3 in Bcl-2–positive cells, there was a small but insignificant ($P > 0.10$) reduction in the percentage of cells developing a transient Ca^{2+} elevation (i.e., one or two Ca^{2+} spikes; Fig. 1 B, left) and a small but insignificant ($P > 0.10$) increase in the percentage of cells developing sustained Ca^{2+} oscillations (i.e., three or more Ca^{2+} spikes; Fig. 1 B, right). Moreover, the mean amplitude of Ca^{2+} spikes at the lowest anti-CD3 concentration (.33 μg/ml) was higher in Bcl-2–positive than in Bcl-2–negative cells (Fig. 1 C), although this difference was not statistically significant ($P > 0.10$).

As noted in Fig. 1 D, a major difference between the Ca^{2+} elevations induced at high versus low anti-CD3 antibody concentrations was in the duration (i.e., width) of the individual Ca^{2+} peaks. This is illustrated by the representative Ca^{2+} traces in Figs. 2 and 3 and is also documented quantitatively in Fig. 1 D. The mean peak width was 4 min at 20 μg/ml anti-CD3 antibody but <1 min at 2 μg/ml anti-CD3 antibody. Moreover, Bcl-2 did not alter the width of individual Ca^{2+} elevations (either transient induced by high anti-CD3 or transient and oscillatory at low anti-CD3; Fig. 1 D).

Detailed comparisons of Ca^{2+} oscillations induced by low concentrations of anti-CD3 antibody in Bcl-2–negative and –positive cells are summarized in Fig. 4. To quantitatively compare the oscillatory frequency in Bcl-2–positive and –negative cells, Ca^{2+} traces from numerous experiments were separated into successive 5-min time periods and the number of Ca^{2+} spikes during each period was logged, a method that has been described previously (Bird and Putney, 2005; Fig. 4, A and B).

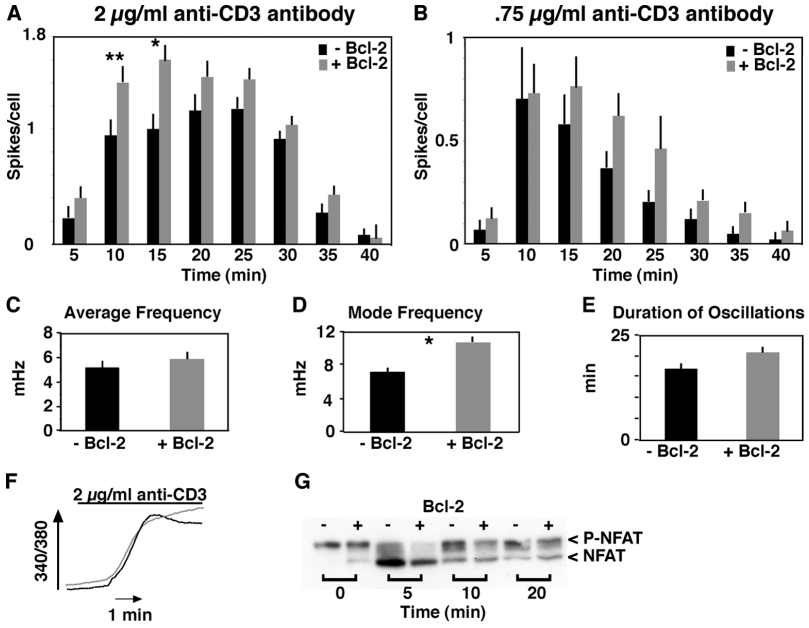

Figure 4. **Comparison of Ca^{2+} oscillations and NFAT activation in Bcl-2–negative and –positive cells.** (A) Cytoplasmic Ca^{2+} was continuously monitored by digital imaging in Bcl-2–negative and –positive cells before and after addition of 2 μg/ml anti-CD3 antibody. Ca^{2+} traces were divided into successive 5-min intervals, and the number of Ca^{2+} spikes per cell in each 5-min interval was recorded as a measure of oscillatory frequency. The analysis was performed on 25 coverslips of Bcl-2–negative cells and 33 coverslips of Bcl-2–positive cells. The frequency of Ca^{2+} spike activity appeared higher in Bcl-2–positive cells at all but the 40-min time period, but the difference between Bcl-2–negative and –positive cells was significant only during the 15-min time period (*, $P = 0.01$) and borderline significant during the 10-min time period (**, $P = 0.057$). (B) The same method of analysis was performed on Ca^{2+} traces at 0.75 μg/ml anti-CD3 antibody, although fewer experiments were performed at this antibody concentration (six coverslips of Bcl-2–negative cells and five coverslips of Bcl-2–positive cells). None of the apparent differences between oscillatory frequency in Bcl-2–negative and –positive cells were statistically significant ($P > 0.10$). (C) The time period between the peaks of individual Ca^{2+} spikes induced by 2 μg/ml anti-CD3 antibody was measured and used to calculate the mean frequency of Ca^{2+} oscillations. The difference between Bcl-2–negative and –positive cells was not significant ($P > 0.10$). (D) The mode frequency of Ca^{2+} oscillations induced by 2 μg/ml anti-CD3 was calculated from the data in C. The mode frequency of oscillations in Bcl-2–positive cells was higher than that in Bcl-2–negative cells (*, $P = 0.01$). (E) The duration of oscillations induced by 2 μg/ml anti-CD3 antibody was measured as the time between the initial and the final Ca^{2+} elevations in an oscillatory run. The apparent difference between the duration of oscillations in Bcl-2–negative and –positive cells was not significant ($P > 0.10$). Error bars represent mean ± SEM. In F and G, suspensions of Bcl-2–negative and –positive cells were treated with 2 μg/ml anti-CD3 antibody. (F) The anti-CD3–induced elevation of cytoplasmic Ca^{2+} was recorded fluorometrically in fura-2–AM–loaded cells (black line, Bcl-2–negative cells; gray line, Bcl-2–positive cells). (G) Immunoblot documenting NFAT activation by 2 μg/ml anti-CD3 antibody, representative of three separate experiments. The top band depicts phosphorylated (inactive) NFAT, whereas the bottom band shows the dephosphorylated (activated) form of NFAT.

Overall, the frequency of Ca^{2+} oscillations induced by 2 μg/ml anti-CD3 antibody appeared higher in Bcl-2–positive than in Bcl-2–negative cells, although differences reached statistical significance only during the 15-min time interval ($P = 0.01$) and borderline significance during the 10-min time interval ($P = 0.057$; Fig. 4 A). The frequency of oscillations also appeared to be higher in Bcl-2–positive cells at 0.75 μg/ml anti-CD3 antibody, but differences were not statistically significant at any of the time intervals (Fig. 4 B). To analyze oscillatory frequency by a different method, the time interval between Ca^{2+} spikes was measured in multiple Ca^{2+} traces at 2 μg/ml anti-CD3 antibody and, based on these data, mean and mode frequencies were calculated. The mean frequency of Ca^{2+} oscillations in Bcl-2–negative cells was 5.2 ± 0.6 mHz, whereas the mode frequency was 7.3 ± 0.55 mHz. Mean frequency was lower than mode frequency because of the presence of low-frequency spiking detected in a small proportion of the Ca^{2+} traces. The mean frequency was not significantly different in Bcl-2–negative and –positive cells (Fig. 4 C), but the mode frequency was significantly higher in Bcl-2–positive cells (Fig. 4 D). Thus, consistent with the analysis in Fig. 4 A, this analysis suggests an increased frequency of Ca^{2+} oscillations in Bcl-2–positive compared to Bcl-2–negative cells. The total duration of Ca^{2+} oscillatory runs (i.e., time duration from initial to final Ca^{2+} spikes) appeared longer in Bcl-2–positive than in Bcl-2–negative cells, although this difference was of borderline significance ($P = 0.05$; Fig. 4 E). WEHI7.2 cells adhered loosely to coverslips, limiting the rate at which anti-CD3 antibody could be perfused onto cells. Therefore, to estimate latency period, the initial Ca^{2+} response to 2 μg/ml anti-CD3 antibody was recorded in cell suspensions fluorometrically (Fig. 4 F). Based on these data, the latency period was on the order of 2 min and was the same in Bcl-2–negative and –positive cells. Although the preceding analyses suggest that Bcl-2 may slightly increase the frequency and duration of Ca^{2+} oscillations, the major conclusion from these data is that Bcl-2 does not inhibit Ca^{2+} oscillations induced by low concentrations of anti-CD3 antibody. Consistent with this finding, Bcl-2 did not inhibit NFAT activation (Fig. 4 G).

Bcl-2 inhibits anti-CD3–induced apoptosis by inhibiting anti-CD3–induced Ca^{2+} elevation

The mean amplitudes of Ca^{2+} elevations induced by high and low concentrations of anti-CD3 antibody were compared in Fig. 1 C. Although the mean peak amplitude of the Ca^{2+} elevation induced by 20 μg/ml anti-CD3 was similar to the mean peak amplitude of Ca^{2+} spikes induced by 2 μg/ml anti-CD3, the net effect of amplitude and width of Ca^{2+} peak is a much more substantial Ca^{2+} elevation after high anti-CD3 than after low anti-CD3. Furthermore, analysis of the peak Ca^{2+} elevation induced by 20 μg/ml anti-CD3 on an individual cell basis illustrates a broad range of Ca^{2+} elevations detected in Bcl-2–negative cells (Fig. 5). 27% of the Ca^{2+} spikes in Bcl-2–negative cells were >200 nM, an arbitrarily chosen threshold level, whereas only 7% of Ca^{2+} spikes in Bcl-2–positive cells were higher than this level after treatment with 20 μg/ml anti-CD3 antibody. Therefore, Bcl-2 not only reduces the percentage of cells that elevate Ca^{2+} in response to high anti-CD3 (Fig. 1 B) but also dampens Ca^{2+} elevations in the cells

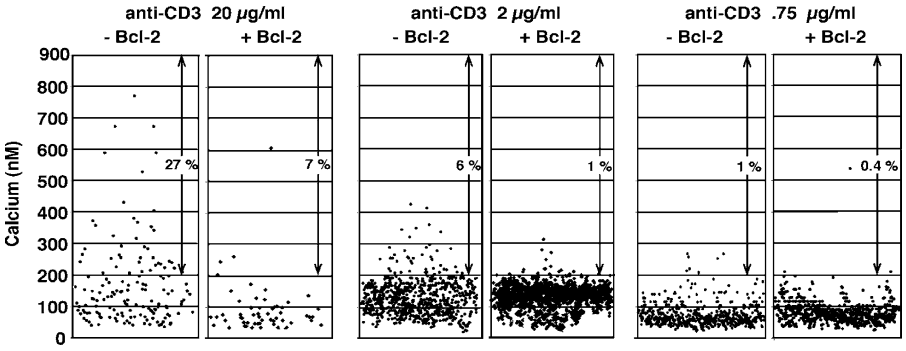

Figure 5. **Bcl-2 dampens Ca^{2+} elevations induced by anti-CD3 antibody.** Peak Ca^{2+} elevations induced by 20 (left), 2 (middle), and 0.75 (right) μg/ml anti-CD3 in Bcl-2–negative and –positive cells are represented by dots, where each dot represents either an individual transient elevation or an individual oscillatory spike, arranged at random on the horizontal axis. The percentage of Ca^{2+} elevations over an arbitrary threshold of 200 nM is shown. Ca^{2+} elevations to <40 nM were not recorded. Data are from multiple experiments (150 elevations for Bcl-2–negative cells at 20 μg/ml; 58 transient elevations for Bcl-2–positive cells at 20 μg/ml; 758 spikes for Bcl-2–negative cells at 2 μg/ml; 1,430 spikes for Bcl-2–positive cells at 2 μg/ml; 559 spikes for Bcl-2–negative cells at 0.75 μg/ml; 692 spikes for Bcl-2–positive cells at 0.75 μg/ml).

that do respond by preventing very high peak Ca^{2+} elevations. In contrast to the wide distribution of Ca^{2+} elevations observed at 20 μg/ml anti-CD3 antibody in Bcl-2–negative cells, only 6 and 1% of Ca^{2+} spikes were >200 nM at 2 and 0.75 μg/ml anti-CD3 antibody in Bcl-2–negative cells (Fig. 5). Even fewer cells elevated their Ca^{2+} to >200 nM at these low concentrations of anti-CD3 antibody in Bcl-2–positive cells (Fig. 5 C). Thus, although Bcl-2 did not reduce the percentage of cells that responded to low concentrations of anti-CD3 antibody by developing sustained Ca^{2+} oscillations (Fig. 1 B) and did not reduce the mean amplitude of these Ca^{2+} elevations (Fig. 1 C), it does appear to have set a threshold level above which the Ca^{2+} does not elevate even in response to weak TCR activation.

To investigate the contribution of high Ca^{2+} elevations to anti-CD3–induced apoptosis, cells were treated with 20 μg/ml anti-CD3 antibody and sorted by flow cytometry into two different populations based on relative levels of cytoplasmic Ca^{2+} (Fig. 6 A). The cells were then placed in culture, and the percentage of apoptotic cells was measured 24 h later. A significantly higher percentage of cells in the high Ca^{2+} population underwent apoptosis, compared to cells in the low Ca^{2+} population (Fig. 6 B). Conversely, reducing extracellular Ca^{2+} concentration, a condition that partially prevents Ca^{2+} elevation after treatment with high anti-CD3 (Fig. 7 A), inhibited apoptosis (Fig. 7 B). Thus, the induction of apoptosis in Bcl-2–negative cells is Ca^{2+} dependent, and the percentage of cells undergoing apoptosis is proportional to the peak amplitude of Ca^{2+} elevation after treatment with a high concentration of anti-CD3 antibody. Consistent with these findings, Bcl-2 inhibited apoptosis induction by high anti-CD3 (Fig. 7, C and D), in accordance with the dampening effect of Bcl-2 on anti-CD3–induced Ca^{2+} elevation described in preceding experiments (Fig. 5). Treatment with low anti-CD3 did not induce apoptosis (Fig. 7 C), consistent with the evidence that high Ca^{2+} elevation (≥200 nM) was much less common after treatment with low anti-CD3 than it was after treatment with high anti-CD3 (Fig. 5). Interestingly, the percentage of apoptotic cells was lower after treatment with low anti-CD3 antibody than it was in untreated cells (Fig. 7 C). This suggests that treatment with low anti-CD3 may have a prosurvival action, in contrast to the proapoptotic action of high anti-CD3.

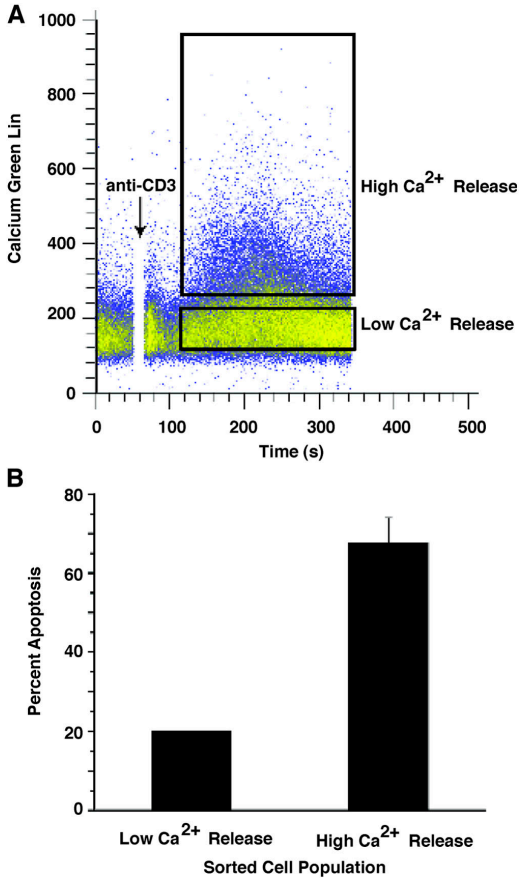

Figure 6. **High levels of Ca^{2+} elevation after anti-CD3 treatment are associated with apoptosis induction.** (A) Bcl-2–negative cells were loaded with the fluorescent Ca^{2+} indicator calcium green and fluorescence (calcium green lin, vertical axis) was monitored continuously by flow cytometry before and after adding anti-CD3 antibody (20 μg/ml). Cells were sorted into two populations corresponding to high and low levels of Ca^{2+} elevation. The high Ca^{2+} group represents 10.7% of the cells sorted, and the low Ca^{2+} group represents 72.8% of the cells sorted. The color gradient represents cellular population density, with yellow representing the area of highest density and blue representing the area of lowest density. (B) After 24 h in culture, sorted cells were stained with Hoechst 33342 and the percentage of cells displaying typical apoptotic nuclear morphology was determined by epifluorescence microscopy. Error bars represent mean ± SEM of two separate experiments.

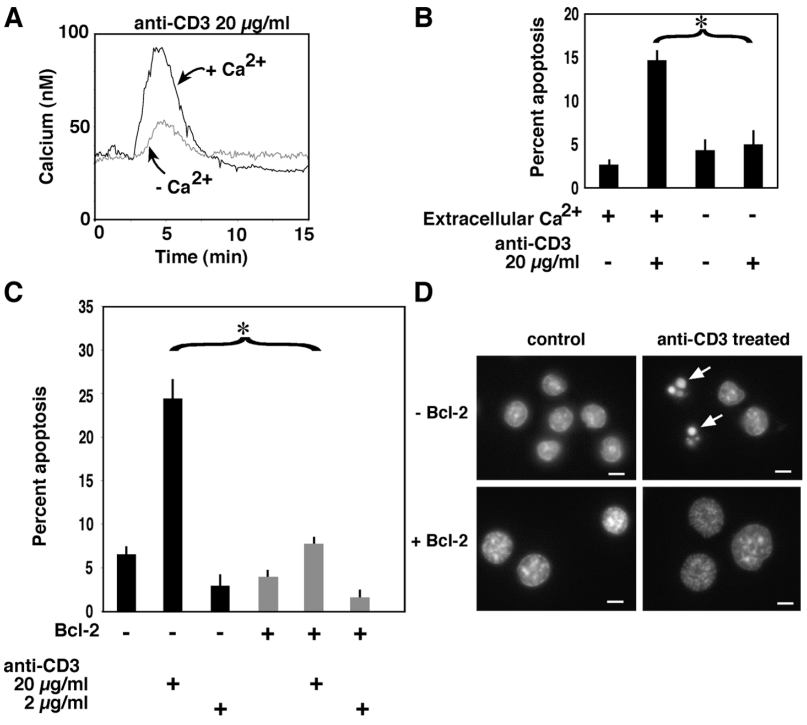

Figure 7. **Bcl-2 inhibits Ca^{2+}-dependent apoptosis induced by high anti-CD3.** (A) Low extracellular Ca^{2+} inhibits anti-CD3–induced Ca^{2+} elevation. Cytoplasmic Ca^{2+} was measured by digital imaging in Bcl-2–negative cells after addition of 20 μg/ml anti-CD3 antibody. Antibody was added during the first 2 min of the trace. The black line depicts the mean Ca^{2+} trace corresponding to 63 cells, with measurements performed in 1.3 mM of extracellular Ca^{2+} buffer, and the gray line depicts the mean Ca^{2+} trace corresponding to 60 cells, with measurements performed in nominally Ca^{2+}-free buffer. (B) Low extracellular Ca^{2+} inhibits anti-CD3–induced apoptosis. Apoptosis was quantified according to nuclear morphological changes as in Fig. 6, 24 h after adding 20 μg/ml anti-CD3 to Bcl-2–negative cells suspended in regular DME (+), which contains 1.3 mM of extracellular Ca^{2+}, or nominally Ca^{2+}-free DME (−). Anti-IgG antibody was added 30 min after anti-CD3 antibody. Error bars represent mean ± SEM in three experiments. The asterisk denotes the significant ($P < 0.01$) inhibitory effect of low extracellular Ca^{2+} on apoptosis induction. (C) In Bcl-2–negative cells, apoptosis is induced by 20 μg/ml anti-CD3 antibody but not by 2 μg/ml anti-CD3 antibody. Bcl-2 inhibits apoptosis induction by anti-CD3 antibody. The percentage of apoptotic cells was determined by epifluorescence microscopy 24 h after adding either 20 or 2 μg/ml anti-CD3 antibody. Anti-IgG antibody was added 30 min after anti-CD3 antibody. Error bars represent mean ± SEM of multiple experiments. The asterisk denotes the significant ($P < 0.01$) inhibitory effect of Bcl-2 on apoptosis induction by 20 μg/ml anti-CD3 antibody. (D) Fluorescence microscopic images of Hoechst 33342–stained cells illustrating the typical apoptotic nuclear morphology induced by 20 μg/ml anti-CD3 antibody in Bcl-2–negative cells. Arrows denote cells having typical apoptotic nuclear morphology. Bars, 5 μm.

Effect of $InsP_3$ receptor knockdown on Ca^{2+} responses to strong and weak TCR activation

To address the question of how Bcl-2 differentially regulates Ca^{2+} signals induced by high versus low concentrations of anti-CD3 antibody, we used small interfering RNA (siRNA) to reduce levels of all three $InsP_3$ receptor subtypes in WEHI7.2 cells (Fig. 8). The siRNA oligonucleotide pools were introduced into cells by electroporation with a transfection efficiency of 78 ± 2% (mean ± SEM). The siRNA-mediated reduction in $InsP_3$ receptor levels was documented by Western blotting (Fig. 8 A). Substantial reduction in all three $InsP_3$ receptor subtypes was reproducibly achieved (Fig. 8 B). This reduction in $InsP_3$ receptors significantly inhibited the Ca^{2+} elevation induced by 20 μg/ml anti-CD3 antibody (Fig. 8, C and D). But the siRNA-mediated reduction in $InsP_3$ receptor levels did not inhibit Ca^{2+} responses to 2 μg/ml anti-CD3 antibody. This is documented by representative Ca^{2+} traces (Fig. 8, E and F), by analysis of the percentage of responding cells (Fig. 8 G), and by amplitude analysis (Fig. 8 H). Thus, consistent with the inhibitory effect of Bcl-2 on Ca^{2+} responses to strong but not to weak TCR activation, the former appears to be more dependent on $InsP_3$ receptor expression levels than the latter.

Discussion

The principal finding in this study is that Bcl-2 differentially regulates Ca^{2+} signaling in T cells according to the strength of TCR activation. Bcl-2 was found to inhibit the cytoplasmic Ca^{2+} elevation induced by a high concentration of anti-CD3 antibody but did not inhibit Ca^{2+} elevation induced by low concentrations of anti-CD3 antibody. This finding evolved as a natural extension of our earlier investigation into the effect of Bcl-2 on $InsP_3$ receptor–mediated Ca^{2+} release from the ER (Chen et al., 2004). Those studies initially used fluorometric measurements of Ca^{2+} elevation in response to a relatively high concentration of anti-CD3 antibody. It was this Ca^{2+} elevation that we found to be inhibited by Bcl-2. Although digital imaging was eventually used in addition to fluorometry in these earlier studies, a high concentration of anti-CD3 antibody was adhered to throughout. Thus, only the effect of Bcl-2 on the transient Ca^{2+} elevation induced by a relatively high concentration of anti-CD3 antibody was investigated. The present study was undertaken based on the prediction that Ca^{2+} oscillations would be detected if a lower concentration of anti-CD3 antibody were used. This prediction was based on evidence that high concentrations of cell surface receptor agonists generally induce transient elevations of Ca^{2+}, whereas low concentrations of agonist are more likely to induce sustained oscillations (Berridge, 1990). Consistent with this paradigm, it was previously reported that strong TCR activation induces primarily a transient Ca^{2+} elevation, whereas weaker TCR activation induces primarily repetitive Ca^{2+} spikes, or oscillations (Donnadieu et al., 1992a).

As anticipated, the Ca^{2+} response pattern in WEHI7.2 cells underwent a transition from transient Ca^{2+} elevation to sustained oscillations as anti-CD3 antibody concentration was decreased (Fig. 1 A). The Ca^{2+} oscillations induced by anti-CD3 antibody were irregular in their amplitude and frequency (Fig. 3). This is characteristic of Ca^{2+} oscillations in T cells,

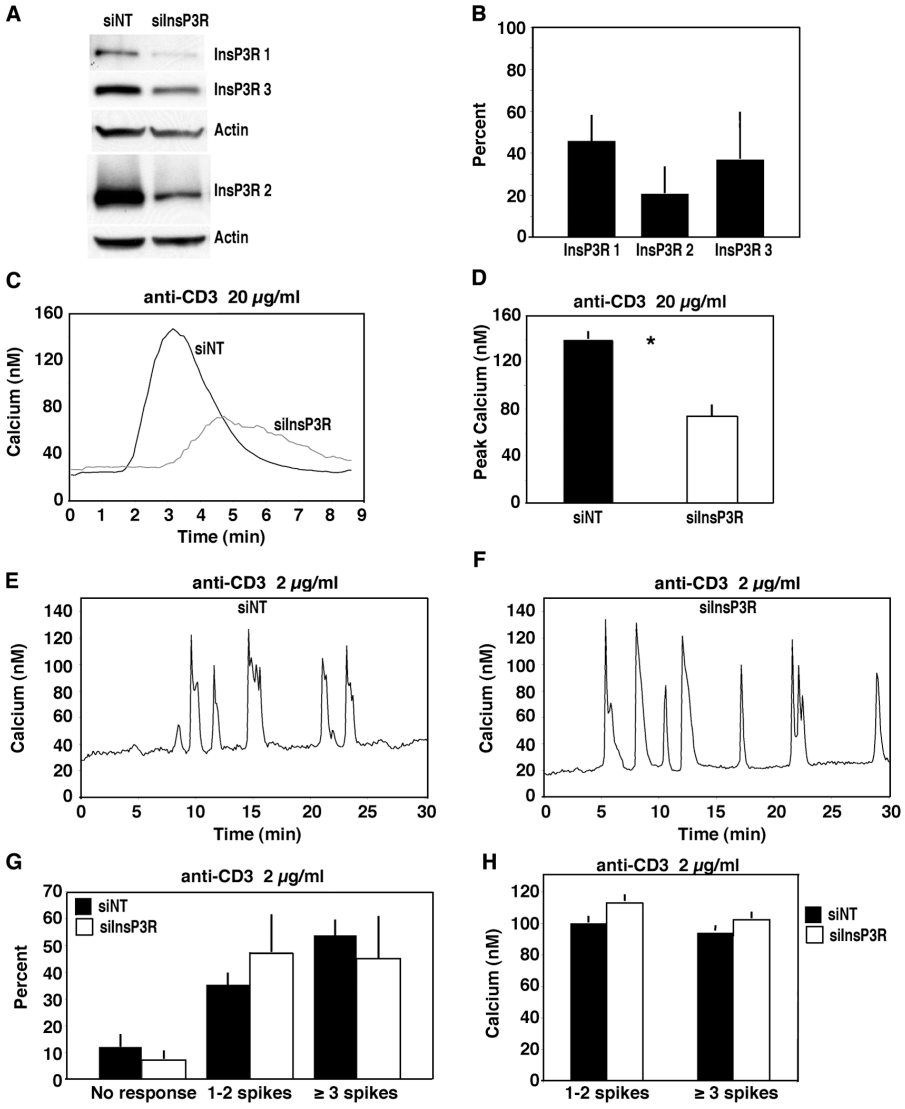

Figure 8. **$InsP_3$ receptor down-regulation inhibits Ca^{2+} elevation induced by high but not low anti-CD3.** (A) Western blot showing levels of $InsP_3Rs$ in WEHI7.2 cells treated with either a nontargeting control siRNA pool (siNT) or siRNA targeted toward all three $InsP_3R$ subtypes ($siInsP_3R$). The level of actin was measured as a loading control. Note that Westerns for types 1 and 3 $InsP_3Rs$ were performed on the same membrane, whereas the Western for type 2 $InsP_3R$ was performed on a different membrane. (B) Densitometric measurement of $InsP_3R$ levels on Western blots, normalized to actin, where the level of $InsP_3R$ after treatment of cells with the $siInsP_3R$ is expressed as a percentage of the level after treatment with control siNT. Error bars represent the mean ± SEM of three separate experiments. (C) Representative Ca^{2+} traces indicating that knocking down $InsP_3R$ levels inhibits the Ca^{2+} elevation induced by 20 μg/ml anti-CD3 antibody. Antibody was added during the first minute of the trace. The data are from experiment 091905 and represent the mean ± SEM of Ca^{2+} in 54 siNT-treated cells and 38 $siInsP_3R$-treated cells. (D) Mean Ca^{2+} elevation in siNT-treated cells and $siInsP_3R$-treated cells induced by 20 μg/ml anti-CD3 antibody. Data are from five experiments in siNT-treated cells (349 cells total) and five experiments in $siInsP_3R$-treated cells (279 cells total). Error bars represent mean ± SEM. *, $P < 0.01$. (E) Representative Ca^{2+} trace from siNT-treated cells, where Ca^{2+} oscillations were induced by 2 μg/ml anti-CD3 antibody. Antibody was added during the first 2 min of the trace. (F) Representative Ca^{2+} trace from $siInsP_3R$-treated cells, where Ca^{2+} oscillations were induced by 2 μg/ml anti-CD3 antibody. (G) The percentage of cells with no response to 2 μg/ml anti-CD3 antibody or with development of 1 or 2 or ≥3 spikes, comparing siNT- and $siInsP_3R$-treated cells. Error bars represent mean ± SEM. None of the differences were significant ($P > 0.10$). (H) The mean amplitude of Ca^{2+} elevations induced by 2 μg/ml anti-CD3 antibody in siNT- and $siInsP_3R$-treated cells. Error bars represent mean ± SEM. None of the differences were significant ($P > 0.10$).

as reported previously by others, and is in contrast to the more uniform pattern of Ca^{2+} oscillations observed in nonlymphoid cells (for reviews see Lewis, 2001; Randriamampita and Trautmann, 2004). The irregularity of anti-CD3–induced Ca^{2+} oscillations necessitated a large number of experiments to objectively compare oscillatory responses in Bcl-2–negative and –positive cells (Fig. 4). The only significant differences were an increase in oscillatory frequency (Fig. 4, A and D) and duration of oscillations (Fig. 4 E) in Bcl-2–positive cells. The oscillatory patterns induced in Bcl-2–negative and –positive cells were indistinguishable in all other respects, including the percentage of cells that developed oscillations (Fig. 1 B), amplitude (Fig. 1 C), width of Ca^{2+} spikes (Fig. 1 D), and latency period (Fig. 4 F). It has been reported that NFAT is optimally activated by Ca^{2+} oscillations (Dolmetsch et al., 1998; Tomida et al., 2003; for reviews see Lewis, 2003; Winslow and Crabtree, 2005). Therefore, NFAT activation was measured as a convenient "readout" of the Ca^{2+} oscillations induced by anti-CD3 in WEHI7.2 cells. Consistent with the finding that Bcl-2 did not inhibit anti-CD3–induced Ca^{2+} oscillations, Bcl-2 did not inhibit NFAT activation (Fig. 4 G).

The finding that Bcl-2 selectively inhibits the transient Ca^{2+} elevation induced by high anti-CD3 without interfering with Ca^{2+} oscillations induced by low anti-CD3 is relevant to the role of Bcl-2 in regulating apoptosis, as WEHI7.2 cells undergo apoptosis after treatment with high anti-CD3 but not when treated with low anti-CD3 (Fig. 7 C). Moreover, apoptosis induction by high anti-CD3 was Ca^{2+} mediated (Fig. 7, A and B), and the percentage of cells undergoing apoptosis was proportional to the level of Ca^{2+} elevation (Fig. 6). These findings are consistent with evidence that apoptosis induction after TCR activation is triggered by $InsP_3$ receptor–mediated Ca^{2+} elevation (Nakayama et al., 1992; Jayaraman and Marks, 1997). Thus, by selectively repressing the Ca^{2+} elevation induced by strong TCR activation, Bcl-2 inhibits apoptosis without interfering with physiological Ca^{2+} signals induced by weak TCR activation.

The present findings are intriguing in light of the known role of Bcl-2 in T cell development. T cells located in the thymic cortex are TCR positive and both CD4+ and CD8+ ("double positive"). At this stage of T cell development, Bcl-2 expression is low and cortical thymocytes are highly susceptible to apoptosis induction after TCR activation by antigen or anti-CD3 antibody (Smith et al., 1989; Murphy et al., 1990; Shi et al., 1991; Nakayama et al., 1992). When T cells mature and migrate to the thymic medulla, they remain TCR positive but become either CD4+CD8− or CD4−CD8+ ("single positive"). Bcl-2 expression is increased at this stage of development, and as a consequence, single-positive thymocytes are less susceptible to apoptosis than are cortical thymocytes (Gratiot-Deans et al., 1993; Veis et al., 1993). A strong correlation has been demonstrated between Bcl-2 expression and susceptibility to Ca^{2+}-induced apoptosis during T cell development (Andjelic et al., 1993). Thymocytes at the earliest stage of development (TCR−CD4−CD8−), the stage during which thymocytes relocate from bone marrow to thymus, express high levels of Bcl-2 and are resistant to Ca^{2+}-mediated apoptosis, whereas thymocytes in the next stage of development (TCR+CD4+CD8+) are highly susceptible to Ca^{2+}-mediated apoptosis. It is in this stage of development that thymocytes undergo either negative or positive selection. Strong ligation of the TCR (e.g., by self-peptide–major histocompatibility complex [MHC] complexes) induces negative selection, whereas weak ligation of the TCR (e.g., by foreign antigen–MHC complexes) induces positive selection (for review see Hogquist, 2001; Neilson et al., 2004). Double-positive thymocytes from Bcl-2–transgenic mice accumulate excessively because of reduced negative selection and are resistant to anti-CD3–induced apoptosis (for review see Cory, 1995). Therefore, the role of Bcl-2 expression during T cell development may be to regulate when and where negative selection occurs. Decreased Bcl-2 expression in double-positive cortical thymocytes, but not in earlier or later stages of T cell development, may limit negative selection to the cortical region of the thymus and to this stage of development. Elevated Bcl-2 expression at earlier (double negative) and later (single positive) stages of T cell development may dampen Ca^{2+} transients produced by strong TCR engagement while permitting repetitive Ca^{2+} oscillations that signal cell proliferation and survival.

The mechanism by which Bcl-2 differentially regulates Ca^{2+} elevation after strong but not weak TCR activation is not entirely understood. In our earlier work (Chen et al., 2004), the inhibitory effect of Bcl-2 on anti-CD3–induced Ca^{2+} elevation appeared to be mediated at the level of the $InsP_3$ receptor rather than in upstream TCR signaling pathways. This conclusion was based on two experimental strategies in which upstream TCR signaling pathways were bypassed. In one strategy, we found that Bcl-2 inhibited Ca^{2+} elevation induced by a cell-permeant $InsP_3$ ester. In the other strategy, we found that Bcl-2 inhibited ER Ca^{2+} release induced by adding $InsP_3$ to cells in which the plasma membrane had been permeabilized by digitonin. In addition, Bcl-2 appeared to interact with $InsP_3$ receptors, based on results of blue native gel electrophoresis and coimmunoprecipitation (Chen et al., 2004). Finally, purified Bcl-2 inhibited $InsP_3$-gated single-channel opening when microsomal membrane fractions containing $InsP_3$ receptors were incorporated into planar lipid bilayers (Chen et al., 2004). Therefore, the collective evidence that Bcl-2 interacts with $InsP_3$ receptors and inhibits $InsP_3$-mediated Ca^{2+} release from the ER raises the question of whether the induction of Ca^{2+} oscillations by low concentrations of anti-CD3 antibody is $InsP_3$ receptor independent or at least requires far fewer functional $InsP_3$ receptors than does the elevation of Ca^{2+} induced by a high concentration of anti-CD3 antibody.

To address this question, we used siRNA to reduce $InsP_3$ receptor levels in WEHI7.2 cells (Fig. 8). This procedure inhibited Ca^{2+} elevation induced by strong TCR activation but did not inhibit the induction of Ca^{2+} oscillations by weak TCR activation. In contrast, Ca^{2+} responses evoked in HeLa cells by both high and low concentrations of ATP or histamine were repressed by $InsP_3$ receptor type 1 knockdown (Hattori et al., 2004). Thus, mechanisms of Ca^{2+} oscillation formation after TCR activation and G protein–coupled receptor activation may differ. Our findings indicate that Ca^{2+} responses initiated by weak TCR activation are generated independent of $InsP_3$ receptor–mediated Ca^{2+} release or that only a relatively small proportion of the full $InsP_3$ receptor complement is required to initiate Ca^{2+} signals in response to weak TCR activation.

In future studies, the mechanism of how Bcl-2 regulates $InsP_3$ receptor function will be addressed in greater depth. In preliminary studies, we found that Bcl-2 overexpression decreases $InsP_3$ receptor phosphorylation in WEHI7.2 cells. Moreover, it has recently been reported that Bcl-2 interacts with $InsP_3$ receptors in a manner that is dependent on the Bcl-2 phosphorylation state and may regulate Ca^{2+} dynamics in the ER through regulation of $InsP_3$ receptor phosphorylation (Bassik et al., 2004; Oakes et al., 2005). Others have reported that in neuronal cells Bcl-2 shuttles calcineurin to $InsP_3$ receptors and regulates Ca^{2+} release from internal stores (Erin et al., 2003a,b; Erin and Billingsley, 2004). Therefore, one hypothesis is that strong TCR signals enhance $InsP_3$ receptor phosphorylation, enhancing $InsP_3$-induced Ca^{2+} release, and that Bcl-2 dampens the Ca^{2+} response to strong TCR activation by mediating dephosphorylation of $InsP_3$ receptors. Although untested, this theory is consistent with evidence that phosphorylation regulates the Ca^{2+} channel activity of $InsP_3$ receptors (Cameron et al., 1995; Jayaraman et al., 1996; deSouza et al., 2002; Straub et al., 2002; Cui et al., 2004).

In summary, we previously discovered that the known antiapoptotic protein Bcl-2 interacts with $InsP_3$ receptors and inhibits $InsP_3$-induced Ca^{2+} release from the ER in T cells. In this paper, we report that Bcl-2 selectively inhibits Ca^{2+} elevation induced by high but not low anti-CD3. As a consequence, Bcl-2 represses the transient elevation of Ca^{2+} associated with apoptosis induction after strong TCR activation but does not interfere with Ca^{2+} oscillations that activate NFAT after weak TCR activation. The capacity of Bcl-2 to differentially regulate Ca^{2+} signals induced by strong versus weak TCR activation allows Bcl-2 to selectively inhibit apoptotic Ca^{2+} signals without interfering with Ca^{2+} signals that mediate cell proliferation and survival.

Materials and methods

Reagents

EGTA and standard reagents were purchased from Sigma-Aldrich. Fura-2–AM and Hoechst 33342 were purchased from Invitrogen. Hamster anti–mouse CD3e ε chain monoclonal antibody (clone 145-2C11) and mouse anti–hamster IgG1 monoclonal antibody were obtained from BD Biosciences. Mouse monoclonal antibody NFATc2 was obtained from Santa Cruz Biotechnology, Inc.

Cell culture

WEHI7.2 cells were cultured in DME supplemented with 10% bovine calf serum, 2 mM L-glutamine, and 100 μM of nonessential amino acids. Transfection procedures, isolation of Bcl-2–positive and –negative clones, and the characterization of these clones were reported previously (Chen et al., 2004).

Ca^{2+} imaging

Methods of Ca^{2+} imaging, described in detail previously (Chen et al., 2004), were used here with only minor modifications. In brief, cells adhered to poly-L-lysine–coated coverslips (35-mm coverslip dishes; MatTek Corp.) were loaded with 1 μM fura-2–AM for 45 min at 25°C in extracellular buffer (ECB; 130 mM NaCl, 5 mM KCl, 1.5 mM $CaCl_2$, 1 mM $MgCl_2$, 25 mM Hepes, pH 7.5, 1 mg/ml BSA, and 5 mM glucose). The buffer was replaced with fresh ECB and the incubation was continued for 45 min at 25°C to permit deesterification. Culture dishes were mounted on the nonheated stage of an inverted microscope (CKX41; Olympus) equipped with a 20× fluor objective. Excitation light was alternated between 340 and 380 nm by a filter wheel (Sutter Instrument Co.), with 0.8- and 0.2-s exposure times, respectively, and emitted light was filtered at >510 nm and collected with an intensified charge-coupled device camera (12-bit VGA; Cooke). Anti-CD3 antibody was gently added to buffer overlaying the coverslip so as not to disturb cells loosely adherent to the coverslip. The video signal was digitized using InCyt Im2 software (Intracellular Imaging) and subsequently processed using Excel (Microsoft). To determine R_{min}, cells were perfused with ECB deficient in Ca^{2+} and supplemented with 4 mM EGTA and 10 μM ionomycin. R_{max} was obtained by perfusing cells with ECB supplemented with 4 mM $CaCl_2$ and 10 μM ionomycin. Ca^{2+} concentration was calculated based on the published K_d for fura-2 of 220 nM, by the equation of Grynkiewicz et al. (1985).

Fluorometric Ca^{2+} measurements

The measurement of Ca^{2+} concentration in cell suspensions by fluorometry using fura-2–AM have been described in detail previously (Chen et al., 2004).

NFAT Westerns

Cells were treated with 2 μg/ml anti-CD3 antibody for various time periods at ambient temperature, after which they were placed on ice, pelleted, and resuspended in RIPA buffer (1% Triton X-100, 0.1% SDS, 50 mM Tris, pH 7.6, 150 mM NaCl, and 200 mM DTT) supplemented with Complete mini protease inhibitors (Roche) and Phosphatase inhibitor cocktails I and II (Sigma-Aldrich). Cell extracts were resolved by electrophoresis on 7% SDS–polyacrylamide gels under reducing conditions. The separated proteins were transferred to Immobilon-P PVDF membranes (Millipore) and incubated with anti-NFATc2 antibody at a dilution of 1:500, followed by incubation with horseradish peroxidase–conjugated goat anti–mouse IgG and visualized by the ECL Western blotting detection reagent (GE Healthcare).

$InsP_3$ receptor Westerns

Western analysis for $InsP_3$ receptors was performed as described previously (Chen et al., 2004). Protein samples were extracted as in the preceding method and resolved (60 μg/lane) through 4–20% gradient gels (Bio-Rad Laboratories). The antibodies for types 1 and 3 $InsP_3$ receptors were purchased from EMD Biosciences and BD Biosciences, respectively. The antibody for type 2 $InsP_3$ receptor was a gift from R. Wojcikiewicz (State University of New York Upstate Medical University, Syracuse, NY). The antibody for actin was obtained from Sigma-Aldrich. Secondary antibodies were obtained from GE Healthcare.

Apoptosis assay

Cells were stained with Hoechst 33342 (final concentration 10 μg/ml), and typical apoptotic nuclear morphology was detected by epifluorescence microscopy using a microscope (Axiovert S100; Carl Zeiss MicroImaging, Inc.) equipped with a 63× oil/1.4 NA plan apochromat objective (Carl Zeiss MicroImaging, Inc.) and a filter cube (model XF23; Omega Optical; excitation = 485 nm, emission = 535 nm). Images were taken on a charge-coupled device camera (ORCA C4742-95-cooled; Hamamatsu) operating with Simple PCI software (Compix, Inc.).

Flow cytometry

Cells (1 million/ml) were loaded with 5 μM calcium green–AM (Invitrogen) for 45 min at 37°C in ECB. The cells were then pelleted and resuspended in ECB at the same concentration and incubated at room temperature for 30 min to allow dye deesterification. The cells were then pelleted and concentrated to 5 million/ml. The cells were then analyzed and sorted on a flow cytometer (Epics Elite; Beckman Coulter). Calcium green fluorescence was measured after dye excitation with a 488-nM argon laser, and emitted light collection was measured through a 525-nM band-pass filter. The cells were initially run through the flow cytometer for 1 min to assess basal cytosolic Ca^{2+}, and 20 μg/ml anti-CD3 antibody was then added. The cells were gated and sorted into two populations: cells with a high level of Ca^{2+} elevation and cells with a low level of Ca^{2+} elevation. The sorted cells were pelleted and resuspended in fresh culture medium and 20 μg/ml anti-CD3 antibody was re-added, and 30 min later an equal concentration of anti–hamster IgG was added. Apoptosis was measured 24 h later, as described in the previous section.

RNA interference

The negative control, siCONTROL Non-Targeting siRNA Pool, and siGENOME SMARTpools for all three subtypes of $InsP_3$ receptor were purchased from Dharmacon. After suspension in 1× siRNA buffer, SMARTpools were added at a concentration of 1 μM each to 0.2-cm cuvettes containing 5 million WEHI7.2 cells suspended in 200 μl Opti-MEM I (Invitrogen). Cuvettes were then subjected to a single 140V 10-ms^2–wave pulse from a GenePulser Xcell (Bio-Rad Laboratories), and the contents of the cuvette were immediately added to fresh media. Cells were grown in culture after transfection for 48 h before use in experiments. Transfection efficiency was measured by transfecting siGLO Cyclophilin (Dharmacon) at a concentration of 1 μM. After 30 min, cells were pelleted and then resuspended in phosphate-buffered saline. Cells were visualized by fluorescence microscopy, with excitation at 546 nm, and at least 200 cells were counted in three separate experiments to determine the percentage of transfected cells.

Statistical analysis

Comparisons were made using the two-tailed *t* test for two samples, assuming equal variance.

The authors especially thank Michael Berridge for suggesting the use of low anti-CD3 concentrations to trigger calcium oscillations and for critical comments and suggestions during the course of this work. The authors also thank William Schilling, George Dubyak, Martin Bootman, Llewelyn Roderick, Gary Bird, and Doug Green for helpful discussions and advice. We thank Michael Sramkoski and Tammy Stefan for assistance with flow cytometry and Richard Wojcikiewicz for providing antibodies.

This work was supported by National Institutes of Health grants RO1 CA085804 (to C.W. Distelhorst) and T32 HL07147 (to M.C. Davis).

Submitted: 29 June 2005
Accepted: 21 November 2005

References

Andjelic, S., N. Jain, and J. Nikolic-Zugic. 1993. Immature thymocytes become sensitive to calcium-mediated apoptosis with the onset of CD8, CD4, and the T cell receptor expression: a role for *bcl-2*? *J. Exp. Med.* 178:1745–1751.

Bassik, M.C., L. Scorrano, S.A. Oakes, T. Pozzan, and S.J. Korsmeyer. 2004. Phosphorylation of Bcl-2 regulates ER Ca^{2+} homeostasis and apoptosis. *EMBO J.* 23:1207–1216.

Berridge, M.J. 1990. Calcium oscillations. *J. Biol. Chem.* 265:9583–9586.

Berridge, M.J. 1997a. Lymphocyte activation in health and disease. *Crit. Rev. Immunol.* 17:155–178.

Berridge, M.J. 1997b. The AM and FM of calcium signalling. *Nature.* 386:759–760.

Berridge, M.J., M.D. Bootman, and H.L. Roderick. 2003. Calcium signaling: dynamics, homeostasis and remodelling. *Nat. Rev. Mol. Cell Biol.* 4:517–529.

Bhakta, N.R., D.Y. Oh, and R.S. Lewis. 2005. Calcium oscillations regulate thymocyte motility during positive selection in the three-dimensional thy-

mic environment. *Nat. Immunol.* 6:143–151.

Bird, G.S., and J.W. Putney Jr. 2005. Capacitative calcium entry supports calcium oscillations in human embryonic kidney cells. *J. Physiol.* 562:697–706.

Cameron, A.M., J.P. Steiner, A.J. Roskams, S.M. Ali, G.V. Ronnett, and S.H. Snyder. 1995. Calcineurin associated with the inositol 1,4,5-trisphosphate receptor-FKBP12 complex modulates Ca^{2+} flux. *Cell.* 83:463–472.

Chen, R., I. Valencia, F. Zhong, K.S. McColl, H.L. Roderick, M.D. Bootman, M.J. Berridge, S.J. Conway, A.B. Holmes, G.A. Mignery, et al. 2004. Bcl-2 functionally interacts with inositol 1,4,5-trisphosphate receptors to regulate calcium release from the ER. *J. Cell Biol.* 166:193–203.

Cory, S. 1995. Regulation of lymphocyte survival by the Bcl-2 gene family. *Annu. Rev. Immunol.* 13:513–543.

Cory, S., and J.M. Adams. 2002. The Bcl-2 family: regulators of the cellular life-or-death switch. *Nat. Rev. Cancer.* 2:647–656.

Cui, J., S.J. Matkovich, N. deSouza, S. Li, N. Rosenblit, and A.R. Marks. 2004. Regulation of the Type 1 inositol 1,4,5-trisphosphate receptor by phosphorylation at tyrosine 353. *J. Biol. Chem.* 279:16311–16316.

deSouza, N., S. Reiken, K. Ondrias, Y. Yang, S. Matkovich, and A.R. Marks. 2002. Protein kinase A and two phosphatases are components of the inositol 1,4,5-trisphosphate receptor macromolecular signaling complex. *J. Biol. Chem.* 277:39397–39400.

Dolmetsch, R.E., R.S. Lewis, C.C. Goodnow, and J.I. Healy. 1997. Differential activation of transcription factors induced by Ca^{2+} response amplitude and duration. *Nature.* 386:855–858.

Dolmetsch, R.E., K. Xu, and R.S. Lewis. 1998. Calcium oscillations increase the efficiency and specificity of gene expression. *Nature.* 392:933–936.

Donnadieu, E., G. Bismuth, and A. Trautmann. 1992a. Calcium fluxes in T lymphocytes. *J. Biol. Chem.* 267:25864–25872.

Donnadieu, E., D. Cefai, Y.P. Tan, G. Paresys, G. Bismuth, and A. Trautmann. 1992b. Imaging early steps of human T cell activation by antigen-presenting cells. *J. Immunol.* 148:2643–2653.

Erin, N., and M.L. Billingsley. 2004. Domoic acid enhances Bcl-2–calcineurin–inositol-1,4,5-trisphosphate receptor interactions and delayed neuronal death in rat brain slices. *Brain Res.* 1014:45–52.

Erin, N., S.K. Bronson, and M.L. Billingsley. 2003a. Calcium-dependent interaction of calcineurin with Bcl-2 in neuronal tissue. *Neuroscience.* 117:541–555.

Erin, N., R.A.W. Lehman, P.J. Boyer, and M.L. Billingsley. 2003b. *In vitro* hypoxia and excitotoxicity in human brain induce calcineurin–bcl-2 interactions. *Neuroscience.* 117:557–565.

Gratiot-Deans, J., L. Ding, L.A. Turka, and G. Nunez. 1993. bcl-2 proto-oncogene expression during human T cell development. *J. Immunol.* 151:83–91.

Grynkiewicz, G., M. Poenie, and R.Y. Tsien. 1985. A new generation of Ca^{2+} indicators with greatly improved fluorescence properties. *J. Biol. Chem.* 260:3440–3450.

Hajnoczky, G., E. Davies, and M. Madesh. 2003. Calcium signaling and apoptosis. *Biochem. Biophys. Res. Commun.* 304:445–454.

Hanson, C.J., M.D. Bootman, and H.L. Roderick. 2004. Cell signalling: IP_3 receptors channel calcium into cell death. *Curr. Biol.* 14:R933–R935.

Hattori, M., A.Z. Suzuki, T. Higo, H. Miyauchi, T. Michikawa, T. Nakamura, T. Inoue, and K. Mikoshiba. 2004. Distinct roles of inositol 1,4,5-trisphosphate receptor types 1 and 3 in Ca^{2+} signaling. *J. Biol. Chem.* 279:11967–11975.

Hess, S.D., M. Oortgiesen, and M.D. Cahalan. 1993. Calcium oscillations in human T and natural killer cells depend upon membrane potential and calcium influx. *J. Immunol.* 150:2620–2633.

Hogquist, K.A. 2001. Signal strength in thymic selection and lineage commitment. *Curr. Opin. Immunol.* 13:225–231.

Jayaraman, T., and A.R. Marks. 1997. T cells deficient in inositol 1,4,5-trisphosphate receptor are resistant to apoptosis. *Mol. Cell. Biol.* 17:3005–3012.

Jayaraman, T., K. Ondrias, E. Ondriasova, and A.R. Marks. 1996. Regulation of the inositol 1,4,5-trisphosphate receptor by tyrosine phosphorylation. *Science.* 272:1492–1494.

Lewis, R.S. 2001. Calcium signaling mechanisms in T lymphocytes. *Annu. Rev. Immunol.* 19:497–521.

Lewis, R.S. 2003. Calcium oscillations in T-cells: mechanisms and consequences for gene expression. *Biochem. Soc. Trans.* 31:925–929.

Murphy, K.M., A.B. Heimberger, and D.Y. Loh. 1990. Induction by antigen of intrathymic apoptosis of CD4+CD8+ TCRlo thymocytes in vivo. *Science.* 250:1720–1723.

Nakayama, T., Y. Ueda, H. Yamada, E.W. Shores, A. Singer, and C.H. June. 1992. In vivo calcium elevations in thymocytes with T cell receptors that are specific for self ligands. *Science.* 257:96–99.

Neilson, J.R., M.M. Winslow, E.M. Hur, and G.R. Crabtree. 2004. Calcineurin B1 is essential for positive but not negative selection during thymocyte development. *Immunity.* 20:255–266.

Oakes, S.A., L. Scorrano, J.T. Opferman, M.C. Bassik, M. Nishino, T. Pozzan, and S.J. Korsmeyer. 2005. Proapoptotic BAX and BAK regulate the type 1 inositol trisphosphate receptor and calcium leak from the endoplasmic reticulum. *Proc. Natl. Acad. Sci. USA.* 102:105–110.

Orrenius, S., B. Zhivotovsky, and P. Nicotera. 2003. Regulation of cell death: the calcium–apoptosis link. *Nat. Rev. Mol. Cell Biol.* 4:552–565.

Randriamampita, C., and A. Trautmann. 2004. Ca^{2+} signals and T lymphocytes "New mechanisms and functions in Ca^{2+} signaling". *Biol. Cell.* 96:69–78.

Shi, Y.F., R.P. Bissonnette, N. Parfrey, M. Szalay, R.T. Kubo, and D.R. Green. 1991. In vivo administration of monoclonal antibodies to the CD3 T cell receptor complex induces cell death (apoptosis) in immature thymocytes. *J. Immunol.* 146:3340–3346.

Smith, C.A., G.T. Williams, R. Kingston, E.J. Jenkinson, and J.J.T. Owne. 1989. Antibodies to CD3/T-cell receptor complex induce death by apoptosis in immature T cells in thymic cultures. *Nature.* 337:181–184.

Straub, S.V., D.R. Giovannucci, J.I.E. Bruce, and D.I. Yule. 2002. A role for phosphorylation of inositol 1,4,5-trisphosphate receptors in defining calcium signals induced by peptide agonists in pancreatic acinar cells. *J. Biol. Chem.* 277:31949–31956.

Tomida, T., K. Hirose, A. Takizawa, F. Shibasaki, and M. Iino. 2003. NFAT functions as a working memory of Ca^{2+} signals in decoding Ca^{2+} oscillations. *EMBO J.* 22:3825–3832.

Veis, D.J., C.L. Sentman, E.A. Bach, and S.J. Korsmeyer. 1993. Expression of the Bcl-2 protein in murine and human thymocytes and in peripheral T lymphocytes. *J. Immunol.* 151:2546–2554.

Winslow, M.M., and G.R. Crabtree. 2005. Decoding calcium signaling. *Science.* 307:56–57.

Winslow, M.M., J.R. Neilson, and G.R. Crabtree. 2003. Calcium signaling in lymphocytes. *Curr. Opin. Immunol.* 15:299–307.